Journal of Physics: Conference Series **764** (2016) 012011 doi:10.1088/1742-6596/764/1/012011

Thermal treatment of solution–processed nano-sized thin films of molybdenum oxide

M Ganchev*, M Sendova-Vassileva, G Popkirov and P Vitanov

Central Laboratory of Solar Energy & New Energy Sources – Bulgarian Academy of Sciences, 72 Tzarigradsko chaussee, 1784 Sofia

*email: mganchev@abv.bg

Abstract. A solution based deposition method to form nano-sized thin films of molybdenum oxide suitable for photovoltaic device applications is presented. The samples were deposited by spin-coating from molybdenum metal organic precursor solution on soda lime glass substrates. The influence of the process parameters such as spinning regime and concentration of the precursor solutions on the thickness and morphology of the films were investigated. The thermal decomposition of the molybdenum precursor and oxide formation were investigated by differential scanning calorimetry and characteristic patterns showed transitions up to 300^{o}C followed by a zone of stability. Optical spectroscopy measurements in the wavelength range from 300 to 1800 nm presented an increase in transparency when temperature of annealing was raised up to 400^{o}C. Raman scattering analysis revealed the presence of mixed molybdenum oxides. Measurements of the electrical conductivity were performed by the 4-point method.

1. Introduction

Transition metal oxides present a large material basis for research and development in a variety of opto-electronic devices. They possess wide possibilities for tuning their electronic properties and an intrinsic chemical stability against oxidation which makes them attractive for applications in organic electronics such as light emitting diodes (OLED), liquid crystal displays (OLCD), thin film transistors (OTFT) and photovoltaics (OPV) [1]. The perovskite solar cells as devices of particular interest noted a remarkable progress and over the last three years have boosted power conversion efficiency from approximately 10% in 2012 [2] to over 21% today [3]. Similar performance brings these devices very close to the efficiencies of leading commercial technologies. Perovskite solar cells are built in two typical configurations: on meso-structured scaffold wide-band gap oxide semiconductors [3, 4] and as planar construction of thin films on a transparent substrate. The planar configuration, developed as adaptation of concept for polymer organic photovoltaics, includes perovskite absorber film sandwiched between hole and electron-transporting layers, processed by simple solution technologies and without high-temperature treatments and annealing [5]. Very often poly (3, 4-ethilene dioxythiophene): poly (styrene sulfonate) – PEDOT:PSS is used as hole-transport layer. Deposited onto the ITO substrate it has favorable influence on the wettability of the coating solution of the halide perovskite. Later it was taken advantage by this low temperature technology to process perovskite solar cells on flexible substrates [6]. However, the PEDOT: PSS contains an active sulphonic group which can lead to corrosion of the ITO substrate or attack and destroy the perovskite, resulting in deteriorated properties of the devices in the long-term [7]. Several alternatives for PEDOT:PSS were attempted, such as NiO_x [8], graphene oxide [7] and PbS [9].

MoO_3 appears to be a prospective hole-transporting material due to its high general stability, proper electronic properties and non-toxic behavior. Solution processed MoO_x was successfully used in efficient organic polymer photovoltaics structures where a remarkable electrical stability was observed [10]. Occasionally, non-ideal current – voltage characteristics are noticed and more detailed information for electro - physical properties of the structure could be accessed by additional measurements in dark and light conditions [11]. Transport properties and recombination phenomena could be evaluated by investigation of transient processes [12]. Comprehensive research in solution processing and thin films MoOx characterization were performed in [13] and transient dynamics in bulk hetero-junction solar cells with the related material were presented in [14]. In this work we have investigated a solution process for deposition of thin films of MoO_x and evaluated optical, structural and morphological properties after annealing at different temperatures in inert atmosphere.

2. Experimental

Thin films MoO_x were deposited by spin coating at 3000 min^{-1} for 30 sec of precursor solutions of molybdenum (VI) oxide bis (2,4 – pentanedionate) - $MoO_2(AcAc)_2$ (mp 184^{o}C) in absolute ethanol on soda lime glass substrates. Subsequently the samples were annealed at different temperatures in a nitrogen glove box. The deposition stock solution was 184 mM (60 g/l) (M1). For deposition of thinner films diluted blends in the ratio 1:2 (92 mM - M2 (30 g/l)) were used.

Mettler DSC 20 standard cell with TC-10A processor, connected to a PC was used for differential scanning calorimetry. Measurements of the optical transmission and reflection spectra were performed in the interval of 300 – 1800 nm using a Shimadzu UV – 3600 spectrophotometer. Raman spectra excited by a HeNe laser were obtained using a Horiba Jobin Yvon LabRam HR 800 spectrometer.

AFM measurements were carried out in tapping mode using a Multimode V unit by Bruker, Santa Barbara, CA. The image processing was performed using SPIP^{tm} 6.1.0 software. The film thickness and spectral distribution of the refractive index and the extinction coefficient were done on an automatic spectroscopic ellipsometer - M2000D, Woollam.Santa Barbara, CA).

3. Results and discussion

3.1. Structural characterization

Differential Scanning Calorimetry analysis (figure 1) was performed in order to gain an insight of the thermal limits and details of the phase transitions during annealing of the thin films deposited from precursor solutions of molybdenyl acetylacetonate $MoO_2(AcAc)_2$ in absolute ethanol. As it is well known, the melting point (accompanied with decomposition) of the compound is 184^{o}C. Curve (1) was obtained for powder of $MoO_2(AcAc)_2$ and presents two endothermic transitions - the first being at 198^{o}C and the second at 247^{o}C. They could be attributed to the decomposition of $MoO_2(AcAc)_2$ and oxide formation, respectively. A subsequent measurement of the same probe (not shown in Fig.1) had no characteristic features, indicating the irreversibility of the reactions. A sample of $MoO_2(AcAc)_2$ which remained overnight under atmosphere of saturated ethanol vapors in nitrogen atmosphere presented two new peaks, at 98^{o}C and 296^{o}C respectively (curve 2) additional to the transitions at 198^{o}C and 248^{o}C for molybdenyl acetylacetonate (cf. curve 1). The first one at 98^{o}C could be assigned to ethanol releasing while the last one at 296^{o}C denotes the point of cleavage of molybdenum - alcohol bonds [15]. Curves 3 and 4 present DSC data of suspensions of $MoO_2(AcAc)_2$ and absolute ethanol in weight ratio 50:50 and 30:70, respectively. The characteristic endothermic transitions at 98^{o}C, 198^{o}C and 247^{o}C are seen again, but at 298^{o}C an exothermic signal appears which should be assigned to the firing of the solvent. Curve (5) obtained for the solution of 184 mM $MoO_2(AcAc)_2$ in absolute ethanol presented the main transition at 98^{o}C whereas the others are negligible probably because of lower concentration. The presented DSC analysis of the active compound and precursor solution points out the characteristic phase transitions and their respective temperature ranges and could help us to determine the desired regime for thermal annealing.

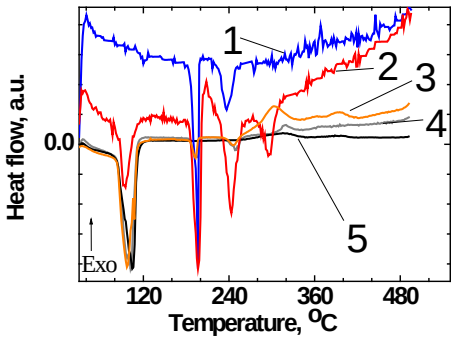

Figure 1. Differential scanning calorimetry: (1) Dry $MoO_2(AcAc)_2$; (2) $MoO_2(AcAc)_2$ under ethanol vapors for 24 hours; (3) 1:1 by weight mix of $MoO_2(AcAc)_2$ and ethanol; (4) 1:3 by weight mix of $MoO_2(AcAc)_2$ and ethanol; (5) Solution of 184 mM $MoO_2(AcAc)_2$ in ethanol.

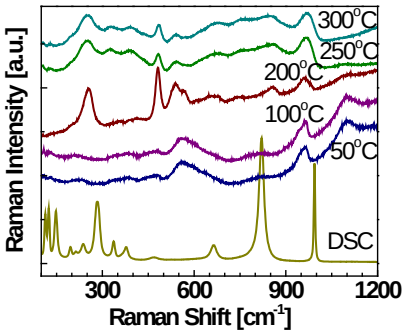

Figure 2. Normalized Raman spectra of MoO_x thin films, deposited with solution M1and annealed in nitrogen at different temperatures shown in the figure as well as of the powder material left after the DSC measurement.

The Raman spectra of the MoO_x thin films, deposited with solution M1 and annealed at different temperatures are shown in figure 2. The spectrum of the powder left after the DSC experiment is shown for comparison. That is a typical spectrum of orthorhombic MoO_3 with clearly visible characteristic bands - 996 cm^{-1} Mo=O stretching, 820 cm^{-1} Mo-O-Mo stretching, 666 cm^{-1} O-Mo stretching, deformation modes below 400 cm^{-1} [16]. The Raman spectra of the films annealed at increasing temperatures exhibit a number of broad bands which could be connected to the evolving disordered molybdenum oxide matrix. At 50ºC and 100ºC only bands in the range 960 – 1100 cm^{-1} and around 560 are observed which could tentatively be assigned to vibrations of Mo=O and Mo-O bonds, respectively, of oxygen atoms bound to a single Mo metal ion [17].

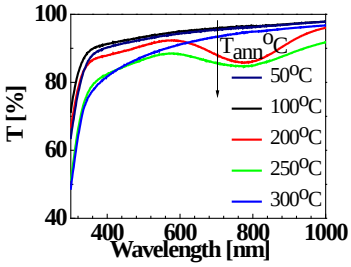

Figure 3. Optical transmission of MoO_x thin films, deposited with solution **M1** and annealed at different temperatures in nitrogen.

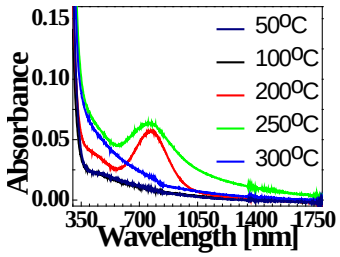

Figure 4. Absorbance of MoO_x thin layers, deposited with solution **M1**and annealed at corresponding temperature in nitrogen.

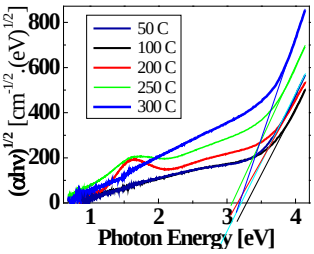

Figure 5. Tauc plot for determination of the band gap of disordered MoO_x thin films.

With increasing temperature bands at around 860 cm^{-1} and one around 255 cm^{-1} appear. The first one could be connected with Mo-O-Mo bonding and the second one to deformational vibrations. The bands between 480 and 580 cm^{-1} acquire more structure at 200ºC. This evolution is evidence of increased structural order and interconnectedness of the MoO_x matrix.

3.2. Optical properties

The deposited thin films demonstrate high transparency (figure 3) which is of great importance for application in solar cells. As shown in the figure the transparency falls a little with the temperature of annealing for the used composition of the precursor solution. After annealing at 200ºC there appears a well formed absorption band at 770 nm (1.6 eV) (cf. figure 4) which is gradually annealed out at higher temperatures. This trend was observed for evaporated layers of MoO_x and the effect is explained with an unstable equilibrium in phase transitions between oxides of Mo^{5+} and Mo^{6+}in this temperature interval[18,19] Figure 5 shows the Tauc plot for assessing the optical band gap of the disordered oxide films. The values obtained are compatible with the literature values for MoO_x thin films.

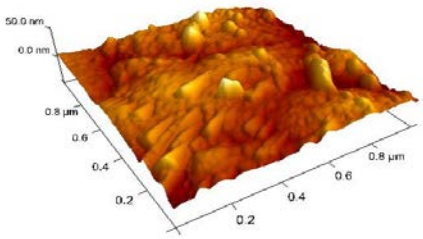

Figure 6. AFM picture of a MoO_x thin film, deposited with solution M1, annealed at 300°C in nitrogen.

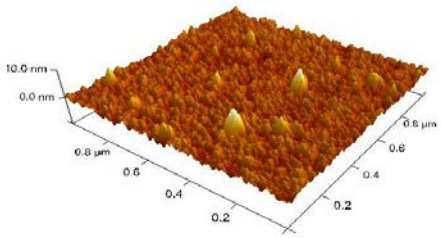

Figure 7. AFM picture of MoO_x thin film,deposited with solution M2 annealed at 200°C in nitrogen (Rq-0.8 nm).

3.3. Morphological characterization

Figure 6 presents the AFM image of sample MoO_x thin film, deposited with solution 184 mM $MoO_2(AcAc)_2$ in ethanol and annealed at 300°C in nitrogen. The estimated (average) grain size is about 200 nm x 40 nm and the root mean square (RMS) value of the surface roughness is about 5 nm. Deposition from diluted solutions leads to formation of flat and more uniform films. Figure 7 presents the AFM image of a MoO_x thin film, deposited from a diluted solution of 92 mM $MoO_2(AcAc)_2$ in ethanol and annealed at 200°C in nitrogen. Significantly lower values of the grain size (about 130 nm x 20 nm) and RMS surface roughness (1.0 ± 0.3 nm) were obtained for annealing temperatures in the range 100°C ÷ 250°C.

Table 1. Sheet resistance of MoO_x thin films, deposited with solutions of 184 mM(M1) and 92 mM (M2) $MoO_2(AcAc)_2$ in ethanol and annealed in nitrogen.

M1 Temp, °C	**sheet resistance, Ω/□.**	**Thickness, nm**	**M2 Temp, °C**	**sheet resistance, Ω/□**
50	265	56	50	
100	260	54	100	
200	380	58	200	260
250	277	58	250	321
300	258	34	300	n.a.

3.4. Ellipsometry and electrical properties

Spectral ellipsometric data (cf. figure 8) were used to determine the thickness of MoO_x films, deposited with solution M1. The values are summarized in Table 1 together with the data for estimated sheet resistances of the related layers.

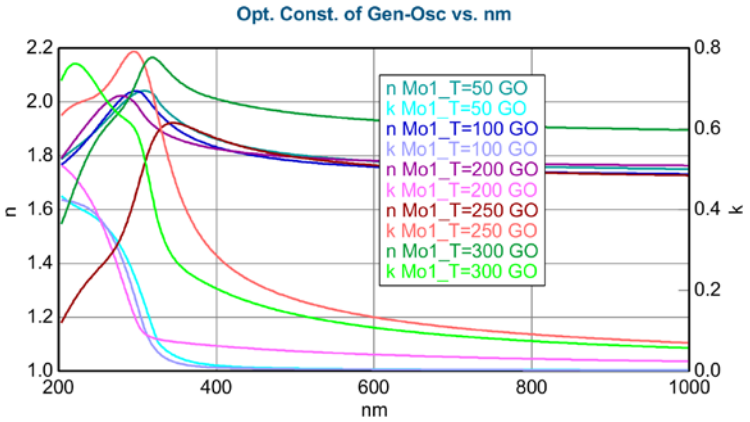

Figure 8. Dispersion of Refractive index and Extinction coefficient of MoO_x thin films, deposited with solution **M1** and annealed at different temperatures in nitrogen.

The sample deposited with concentrated stock solution and annealed at 300°C has remarkably lower thickness. This is probably due to the total desolvation and recrystalization of the MoO_x films. All samples show p-type conductivity and sheet resistance in the range of 260 – 380 Ω/□. Taking into account, that the resistivity $\rho = R_{sheet}$ x *film thickness* and using the data from table 1, we obtain values in the range of 10^{-5} Ω.cm, i.e. thin films of MoO_x could perform as excellent hole-conducting layers.

The spectral distribution of the refractive index and the extinction coefficient for samples deposited with solution 184 mM $MoO_2(AcAc)_2$ in ethanol and annealed at related temperatures in nitrogen is presented in figure 8. Estimated region for beginning of the strong absorption from curves of extinction is before 400 nm which coincides with the data for optical absorbance in figure 4.

Conclusions

The data obtained from DSC analysis of the active compound molybdenum (VI) oxide bis (2,4 – pentanedionate) and its related solutions with absolute ethanol were used to establish the regime for thermal treatments to form MoO_x thin films. Raman scattering have shown gradual desolvation and recrystalization of the layers and formation of definite orthorhombic MoO_3 at temperatures far above 300°C. Elaborated optical investigations revealed high transparency over 90 % with negligible fall near 770 nm (1.6 eV) for temperatures of annealing between 200 – 250°C and a recovery at higher temperatures. Estimated band gap of disordered MoO_x films was about 3.1-3.3 eV. The AFM data have shown decrease of grain sizes of thin MoO_x films with increasing of the annealing temperature and RMS surface roughness about1.0 ± 0.3 nm (as in [13]). The electrical measurements indicated definite p-type conductivity and sheet resistance of the respective thin films in the range 260 – 380 Ω/□. The obtained results show that the properties of solution processed MoO_x thin films are appropriate for application in organic solar cells.

Acknowledgements

This work was supported by Bulgarian National Science Foundation under contract TO2 – 12/ 12.12.2014. Authors express gratitude to Dr I.Bineva for AFM and Dr P.Terzijska for ellipsometric measurements in association with INERA.

References

[1] Yu Wei Su, Shang Che Lan and Kung Hwa Wei. Organic photovoltaics, 15 *Materials today* **12** 554
[2] Kim H-S, Lee C-R, Im J-H, Lee K-B, Moehl T, Marchioro A, Moon S-J, Humphry-Baker R, Yum J-H, Moser JE, Gratzel M and Park N-G 2012 *Sci. Rep.* **2** 591
[3] Jacobsson T J, Correa-Baena J-P, Pazoki M, Saliba M, Schenk K, Gratzel M and Hagfeldt A, 2016 *Energy & Environ. Sci.* **9** 1706
[4] Yang W S, Noh J H, Jeon N J, Kim Y C, Ryu S, Seo J and Seok S Il, 2015 *Science* **348** 6240 1234
[5] Jeng J-Y, Chiang Y-F, Lee M-H, Peng S-R, Guo T-F, Chen P and Wen T-C 2013 *Adv.Mater.* **25** 3727
[6] Docampo P, Ball JM, Darwich M, Eperon GE and Snaith KJ 2013 *Nat.Commun.* DOI: 10.1038/ncomms3761
[7] Yeo JS, Kang R, Lee S, Jeon YJ, Myoung N, Lee CL, Kim DY, Yun JM, Seo YH, Kim SS and Na SI, 2015 *Nano Energy* **12** 96
[8] Kim JH, Liang PW, Williams ST, Cho N, Chueh CC, Glaz MS, Ginger DS and Ken AKY, 2015 *Adv.Mater.* **27** 695
[9] Hu L, Wang W, Liu H, Peng J, Cao H, Shao G, Xie Z, Ma W and Tang J 2015 *J.Mater.Chem.* A **3** 515
[10] Zilberberg K, Gharbi H, Behrendth, Trost A S and Riedl T 2012 *ACS Appl.Mater.Interfaces* **4** 1164
[11] Kirchartz T, Pieters BE, Kirkpatrick J, Rau U and Nelson J 2011 *Phys.Rev. B* **83** 115209
[12] MacKenzie RCI, Shuttle CG, Dibb GF, Treat N, Hauff E von, Robb MJ, Hawker CJ, Chabinyc ML and Nelson J 2013 *J.Phys.Chem.C* **117** 12407
[13] Jasieniak J, Seifter J, Mates JjoT and Heeger AJ 2012, *Adv.Funct.Mater.* **22** 2594
[14] Tremolet de Villers BJ, MacKenzie RCI, Jasieniak J, Treat ND and Chabinyc ML 2014 *Adv.Energy Mater* **4** 1301290
[15] Uzarevic K, Rubcic M, Radic M, Puskaric A and Cindric M 2011 *Cryst.Eng.Comm* **13** 4314
[16] Seguin L, Figlarz M Cavagnat R and Lassègues J-C 1995 *Spectrochim Acta A* **51** 1323
[17] Jasieniak J J, Seifter J, Jo J, Mates T and Heeger A J 2012 *Adv. Funct. Mate*r. **22** 2594
[18] Werner J, Geissbuhler J, Dabirian A, Nikolay S, Morales-Masis M, De Wolf S, Niesen B, Balif C, *ACS Appl.Mater.&Inter.* DOI : 10.1021/acsami.6b04425
[19] Lefteriotis G, Papaefthimiou S, Yanoulis P and Siokou A 2001 *Thin Solid Films* **384** 298